

## Forward and inverse modelling of canopy directional reflectance using a neural network

ABDELGADIR A. ABUELGASIM, SUCHARITA GOPAL,  
and ALAN H. STRAHLER

Center for Remote Sensing and Department of Geography, Boston University,  
675 Commonwealth Ave, Boston, MA 02215, U.S.A.

*(Received 24 June 1996; in final form 12 August 1997)*

**Abstract.** This article explores the use of artificial neural networks for both forward and inverse canopy modelling. The forward neural modelling paradigm involved training a network for predicting the bidirectional reflectance distribution function (BRDF) of a canopy given the density of the trees, their height, crown shape, viewing, and illumination geometry. The neural network model was able to predict the BRDF of unseen canopy sites with 90% accuracy. Analysis of the signal captured by the model indicates that the canopy structural parameters, and illumination and viewing geometry, are essential for predicting the BRDF of vegetated surfaces. The inverse neural network model involved learning the underlying relationship between canopy structural parameters and their corresponding bidirectional reflectance. The inversion results show that the  $R^2$  between the network predicted canopy parameters and the actual canopy parameters was 0.85 for density and 0.75 for both the crown shape and the height parameters. The results of both forward and inverse modelling suggest that neural networks can model accurately the BRDF of vegetated canopies.

### 1. Introduction

An active area of research for the past two decades has been the mathematical modelling of the interaction between the incident electromagnetic radiation and vegetation canopies in the reflective portion of the spectrum. Canopy modelling allows scientists and researchers to formulate mathematically the different interactions that take place within the canopy. Further, these models serve as a guide to experimentation, have the potential to explore unobserved phenomena, and permit the interpretation of data collected (Kimes 1991).

In recent years considerable effort has been made in the development of ecological models that simulate and predict ecosystem functions. These models describe the interaction between the land surface and climate, hydrologic and biochemical cycles, and energy balance, and require critical inputs about the biophysical characteristics of vegetation as well as their spatial and temporal distribution. Remotely sensed data have been used commonly to obtain and estimate these characteristics (Myneni and Ross 1991).

A widely used technique for the estimation of the biophysical characteristics of vegetation is the application of canopy reflectance models (Li and Strahler 1986). Research in the applications of canopy reflectance models during the past decade has resulted in a considerable improvement in the understanding of the influence of the vegetation parameters in the reflectance of the radiation regime. In particular, research efforts have been directed in understanding the effects of factors such as

illumination and viewing geometry, as well as canopy structure, to the bidirectional reflectance distribution function (BRDF) of terrestrial vegetated surfaces (Li and Strahler 1986, 1992, Kimes 1983, Goel and Deering 1985).

The modelling approach usually adopted in remote sensing is of two types: a forward model and an inverse model. The main goal of forward modelling is to simulate a physical process using a given set of physical parameters. On the other hand, the inverse model infers a set of physical parameters that causes a certain physical process or a particular effect. Canopy models are usually forward models formulated to conform to a particular physical or biological abstraction (Strahler *et al.* 1986). Various modelling paradigms have been attempted in this regard to model the vegetation surface's radiation regime; the most common are geometric optics, radiative transfer, hybrids of these, and numerical simulations (Goel 1987).

The main objectives of this article are to assess and explore the use of artificial neural networks in forward and inverse modelling of the bidirectional reflectance of a forest. The problem of forward and inverse modelling in remote sensing is treated here as a mathematical relationship between a set of input parameters and a set of output parameters, that is canopy parameters and corresponding bidirectional reflectances. Neural networks are useful in this context as they can model the relationship between a set of inputs and outputs without exact specification of the functional form. Multilayer feedforward neural networks learn adaptively by examples to approximate an input–output relation or a mapping function between a canopy's bidirectional reflectance and its structural parameters. The assumption here is that the bidirectional reflectance of a canopy is the function of the geometry of its constituent elements (tree height, size), the spatial distribution of the elements, and the illumination and viewing geometry. This implies that the bidirectional reflectance of the canopy is particular to the canopy's structural parameters, and that canopies with different parameters will exhibit different bidirectional reflectance.

Ideally, to learn such a mapping, a data set containing canopy structural parameters and their corresponding bidirectional reflectance should exist. However, such a data set does not exist, and would be expensive to collect. Our study uses a data set that was simulated using the Li and Strahler geometric-optical mutual shadowing model (1992). The model predicts the bidirectional reflectance of tree canopies based on the geometry of the trees, their spatial distribution, the component signatures of the canopy elements, and the viewing and illumination geometry. The Li and Strahler model is used to generate a large training and testing data set, that is used by the neural network. A total of 2200 canopy sites were simulated for this study using Algorithm for MODIS Bidirectional Reflectance Anisotropy of the Land Surface (AMBRALS) code (Wanner *et al.* 1997).

In the case of forward modelling, the approach involves training a multilayer feedforward neural network to learn the mapping function, or to develop an internal representation, between canopy structural parameters and corresponding bidirectional reflectances. A typical input to the neural network in the forward approach consists of a set of canopy parameters (e.g., mean tree height, canopy density), a set of parameters that describe the illumination and viewing geometry, and a set of parameters that describe the typical spectral signatures of the elements present in the scene (figure 1(a)). In the inverse model, the inputs to the neural network consist of the bidirectional reflectance, a set of parameters that describe the typical spectral signatures of the elements present in the scene, and the set of parameters that describe the illumination and viewing geometry (figure 1(b)). The output from the neural

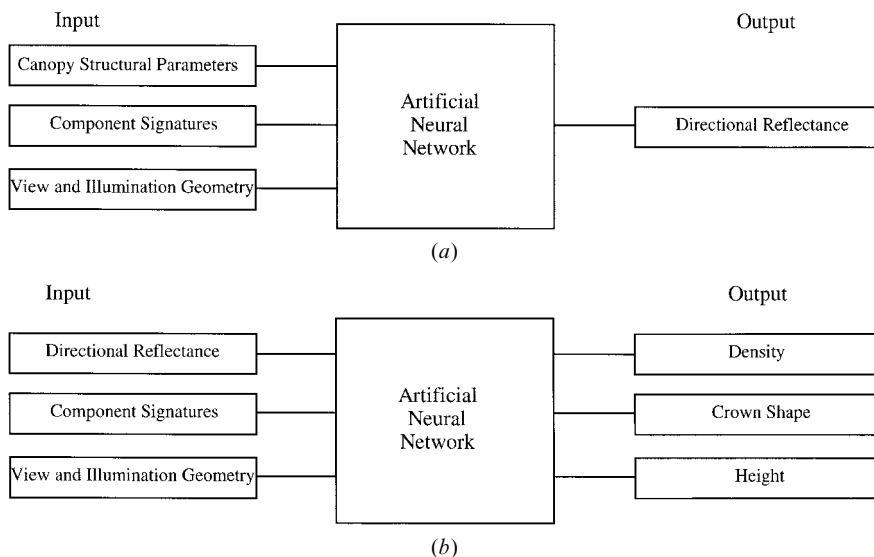


Figure 1. (a) Forward and (b) inverse modelling strategy.

network will be the canopy structural parameters in reference to tree height, size and, density.

## 2. Background

### 2.1. Forward canopy modelling

About two dozen canopy reflectance models have been proposed in the literature, and a comprehensive review is provided by Goel (1987). The models can be categorized into the following main categories.

#### 2.1.1. Radiative transfer models

These models typically treat the medium as a uniform series of plane-parallel horizontal layers. The layers are composed of small absorbing and scattering materials, with defined optical properties, that are randomly distributed and oriented in given directions. Such a modelling paradigm is well suited for establishing the interactions between the radiation and the atmosphere (Chandrasekhar 1950); however, as Myneni *et al.* (1991) noted, in the case of a vegetation canopy, the scattering elements, i.e., leaves, are of finite size, and thus radiative transfer formulations must take this behaviour into account. The shadowing behaviour that produces the hotspot through enhanced single scattering must be accommodated for a radiative transfer model to be realistic (Li and Strahler 1992). Several forms for the treatment of the hotspot function have been attempted, including those of Myneni and Ross (1991), Marshak (1989), Gerstl *et al.* (1986), Myneni *et al.* (1990), Kuusk (1985), Nilson and Kuusk (1989) and Nilson and Peterson (1991). Radiative transfer models are best applied to continuous uniform, vegetated covers, such as crops.

#### 2.1.2. Geometric-optical models

The geometric optical approach models vegetated canopies as discrete three-dimensional objects that are viewed and illuminated from different directions in the hemisphere (Nilson 1977, Li and Strahler 1986). In the geometric optical modelling of Li and Strahler (1985, 1986, 1992), the individual tree canopy was emphasized as

the functional element in modelling. The shape of the objects, their count densities and patterns of placements are the driving variables, and thus condition the mixture of sunlit and shaded objects and background that is observed from a particular view direction, given a certain direction of illumination (Li and Strahler 1986). The combination of this mixture controls the reflectance to a radiometric instrument.

This paradigm of modelling was applied successfully for open and moderately closed tree stands of conifers. Trees were modelled as green spheroids on a contrasting background and illuminated as from a given direction. Li and Strahler (1986) modelled the reflectance associated with a given viewpoint as an area-weighted sum of four fixed reflectance components, namely sunlit leaves or canopy, sunlit background, shaded leaf or canopy, and shaded background.

### 2.1.3. *Hybrid models*

This modelling paradigm presents a hybrid approach between two or more approaches, e.g., radiative transfer models and geometric optical models. The canopy is treated as an assemblage of geometrically shaped plants, where the vegetation elements are considered as scattering and absorbing particles. Multiple scattering is not neglected as in the geometrical approach.

### 2.1.4. *Numerical simulation models*

In these models, the placement and orientation of the vegetated elements are specified, and the interaction between photons and the canopy are simulated by Monte Carlo methods. Vegetation elements are assigned to a finite number of areas, and a Monte Carlo procedure is used to estimate the areas that will interact with the beam of radiation; the interception and scattering of the radiation is numerically followed. Such a procedure has proved to be useful in estimating the spectral reflectance of canopies composed of horizontal inhomogeneous layers of Lambertian surfaces (Smith and Oliver 1974). Kimes and Smith (1980) used a similar approach to estimate the spectral reflectance, absorption and transmittance, and noted good agreement between the model results and the experimental results for a lodgepole pine stand.

Monte Carlo simulations allow the construction of probabilistic models for real processes to estimate certain average characteristics, such as mathematical expectations, variances and covariances (Ross and Marshak 1991). Although they provide good estimates of both the radiation regime within a canopy, and its mean statistical characteristics, such as the probability distribution of the reflected fluxes (Goel 1989), these models are computationally intensive.

## 2.2. *Inverse canopy modelling*

Inversion of canopy reflectance models or, inverse canopy modelling, has been attempted by many researchers. Previous studies have identified two main approaches to infer surface characteristics from the spectral signature; namely the statistical approach and the physical approach. The statistical approach attempts to find a correlation between the objects and their signatures, and then uses statistical techniques to determine the characteristics of an object from its signature (Goel 1989). On the other hand, the physical approach combines the interaction between the incident radiation and the objects into a mathematical model that references the object characteristics and the spectral signature received by the sensor.

Goel (1989) explains that a canopy reflectance model relates the reflectance of a canopy for various solar and viewing directions to the canopy parameters, and that

this relationship can be expressed by the function:

$$y_i = f_i(x_j) \quad (1)$$

for  $i=1, \dots, N$  and  $j=1, \dots, M$ , where  $x_i$  are the  $M$  canopy parameters, and  $y_i$  are the  $N$  canopy reflectances. The inversion strategy is to explore different techniques for the estimation of the inverse of equation (1); that is to express  $x_i$  in terms of the values of  $y_i$ , the bidirectional reflectance.

Modern analytical techniques allow the inversion of complex canopy models through the use of the least squares technique or maximum likelihood under valid conditions and assumptions. Artificial neural networks provide one of the alternative paradigms for learning the underlying relationship between a set of inputs and a set of output parameters. These networks have been applied successfully in inverse problems where the physical parameters that cause a particular effect or physical process can be inferred from remotely sensed data (Zurk *et al.* 1992).

Smith (1993) used multilayer feedforward neural networks for the estimation of leaf area index (LAI) from remotely sensed data. The network was able to map LAI from reflectance and NDVI data with accuracies comparable to that obtained from ground observation. It proved to be more robust than standard regression techniques when applied to varying soil backgrounds. A study by Pierce *et al.* (1994) investigated the use of neural network in inverse modelling of canopy scattering. In this study, the Michigan Microwave Canopy Scattering (MIMICS) model was inverted using an artificial neural network. The results indicated remarkable success in estimating biophysical canopy parameters.

### 3. Data simulations

#### 3.1. The Li and Strahler geometric optical model

This model assumes that canopies consist of three-dimensional tree objects with fixed shape but varying size. Trees are randomly distributed on a contrasting background and are illuminated from a given direction, and viewed from different positions in the hemisphere. A single tree crown is modelled as a simple geometric spheroid, centred at some distance above the ground. A set of fixed form parameters describe the shape of the spheroid to its height, while the height is allowed to vary. The parameter  $b/r$  (the ratio between the radii of the major axis to the minor axis of the crown) describes the crown shape and the parameter  $h/b$  (ratio between height to the centre of crown to the crown's major radius) describes the tree height.

The reflectance of a pixel is assumed to be an area weighted sum of the component signature of four surface components, namely, sunlit crown, sunlit background, shaded crown, and shaded background. The spatial distribution and sizes of the crown determine the proportions of these components within a pixel. Mathematically, the reflectance of a pixel is:

$$R = K_g G + K_c C + K_i T + K_z Z \quad (2)$$

where  $R$  is the reflectance of a pixel;  $G$ ,  $C$ ,  $T$ , and  $Z$  are the spectral signatures of the respective components; and  $K_g$ ,  $K_c$ ,  $K_i$  and  $K_z$  are the areal proportions of sunlit background, sunlit crown, shaded crown and shaded background.

Li and Strahler (1986) modelled the BRDF of a pixel as the limit of its directional

reflectance factor  $R(i, v)$ :

$$R(i, v) = \iint_A \frac{R(s) \langle i, v \rangle \langle v, s \rangle I_i(s) I_v(s) ds}{A \cos \theta_i \cos \theta_v} \quad (3)$$

where  $ds$  is a small Lambertian surface element over area  $A$  of a pixel;  $R(s)$  is the reflectance of  $ds$ ;  $i$ ,  $v$ , and  $s$  represents the directions of illumination, viewing and the normal to a surface element respectively;  $\langle \dots \rangle$  is the cosine of the phase angle between two directions;  $I_i(s)$  and  $I_v(s)$  are indicator functions, equal to one if  $ds$  is illuminated ( $I_i$ ) or viewed ( $I_v$ ) zero otherwise; and  $\theta$  is the zenith angle of a direction. Here the double integral shows that  $ds$  is integrated over the pixel, i.e., the footprint of the sensor's field of view.

To analyse fully the Li and Strahler model, assume that over the pixel area  $A$  there are only two kinds of surfaces, namely, background surface and crown surface with Lambertian reflectance  $G$  and  $C$ , respectively. In this analysis, the area of the background surface that is both illuminated and viewed is denoted as  $A_g$ , and the area of the crown surface both illuminated and viewed is  $A_c$ . Equation (1) can be written as:

$$R(i, v) = K_g G + \frac{C}{A} \iint_A \frac{\langle i, s \rangle \langle v, s \rangle}{\cos \theta_i \cos \theta_v} ds \quad (4)$$

where  $K_g = A_g/A$  is the proportion of background both illuminated and viewed. Considering that the union of  $A_g$  and  $A_c$  is the intersection of the set of surface elements that are illuminated and the set of those that are viewed, only when  $v$  and  $i$  coincide can  $A_g$  and  $A_c$  achieve a maximum, provided that the surface elements have no spatial orientation preference. Thus the hotspot is well explained by this equation. In addition, equation (2) shows that the directional reflectance of the scene depends on the spatial structure that determines  $A_g$  and  $A_c$ , as well as the material reflectance related to  $G$  and  $C$ .

The first term in equation (2) explains that as viewing and illumination coincide, the sunlit background proportions proceed to a maximum; the second term shows that the sunlit crown surface becomes maximally exposed to view at the hotspot. The sunlit surface is assumed to be composed of Lambertian facets. In the Li and Strahler (1992) model, a simple approximation accounts for the mutual shadowing effect. Mutual shadowing occurs when either illumination or viewing assumes directions near the horizon. In such a case, the shadows of the spheroids will fall particularly on the lower portions of neighbouring spheroids, and thus a smaller portion of shaded components is observed. Their approach applies one-stage geometric optics to deal with the spatial relationship between the part of the crown surface that is mutually shaded in the illumination direction and the part mutually shaded in the view direction. For more details, see Li and Strahler (1992).

### 3.2. Simulations

In the present study, the Li and Strahler model is used to generate a data set consisting of bidirectional reflectances that are typical of canopies given their tree geometry and spatial distribution. Initially, 2200 canopy sites are simulated for the study, each site having its unique tree geometry and density. In selecting the tree parameters, reasonable values are used for three vegetation covers: (a) conifer forests, (b) savanna, and (c) shrubland (figure 2). The conifer forests are modelled as a

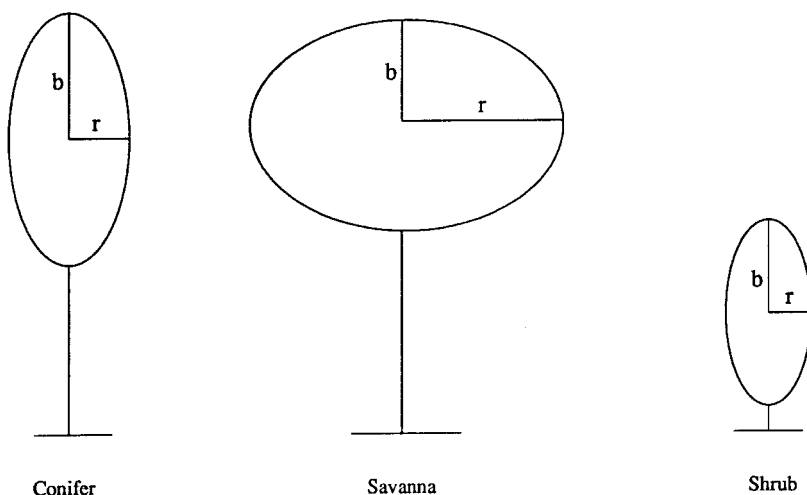


Figure 2. The shape of the three tree canopies simulated.

collection of tall spheroidal crowns, the savanna tree shapes as flattened spheroids, while the shrubs are modelled as spheroids almost resting on the ground. Each canopy site has a varying cover percentage to insure a wide variability of typical realistic densities (see table 1).

In calculating the model's BRDFs for these vegetation covers, the sun illumination angle is varied from  $15^\circ$  to  $60^\circ$  at increments of  $5^\circ$ , resulting in a total of 10 illumination angles. These sun angles are thought to be realistic for satellite sensing scenarios that would include overpasses in mid-morning to mid-afternoon in all seasons of the year. Component signatures are chosen to be similar to reflectance signatures in the red band. The values selected are typical of the reflectance observed in this region of the spectrum for plant matter and soil. In the red band the sunlit crown is usually darker than the sunlit background. Note that in the simulation process the shaded background signature and shaded crown are assumed the same. To insure accurate approximations for the vegetation cover BRDFs, component signatures values are kept constant for each sun angle (table 2).

The 2200 canopy sites are divided into 10 groups insuring that every group contains the maximum variability of the tree parameters. For each group the BRDF is calculated with the Li and Strahler model using one of the ten illumination sun angles and the set of component signatures assigned *a priori* to that angle. The results from the model are the bidirectional reflectance of each tree canopy site in the principal plane and the cross principal plane at viewing angle increments of  $15^\circ$ , i.e., from  $+60^\circ$  in the backscattering direction to  $-60^\circ$  in the forescattering direction.

The model-generated bidirectional reflectances, and the associated canopy sites

Table 1. Canopy parameters of the simulated sites.

Parameter	Minimum	Maximum
Density	8%	100%
Crown shape ratio	0.3	5.2
Height ratio	0.2	6.0

Table 2. Component signatures used in the simulations.

Illumination angle ( $^{\circ}$ )	Sunlit crown signature	Sunlit ground signature	Shaded ground (canopy)
15	0.2190	0.2709	0.0987
20	0.1987	0.2809	0.0456
25	0.1809	0.2906	0.0789
30	0.1679	0.2983	0.0679
35	0.2098	0.3098	0.0981
40	0.1901	0.2698	0.0811
45	0.1523	0.2456	0.0599
50	0.1399	0.2701	0.0509
55	0.1321	0.2374	0.0501
60	0.1897	0.2987	0.0467

form parameters and densities are divided into a training data set and a testing data set for the neural network modelling. The training and testing data set consists of 2000 and 200 observations respectively.

### 3.3. Input data preprocessing

The data used in this study consist of reflectance values, component signatures and canopy parameters. In the forward modelling context, there are eight inputs to the neural network, representing the density, crown shape, height, height distribution within the canopy, sunlit crown signature, sunlit background signature, and shaded crown signature. The output layer consists of 18 units, the first nine representing the bidirectional reflectance of the canopy in the principal plane, from  $+60^{\circ}$  in the backscattering direction to  $-60^{\circ}$  in the forescattering direction at increments of  $15^{\circ}$ . The remaining nine output units represent the bidirectional reflectance across the principal plane.

In the inverse modelling context, there are 22 input units, and three output units. The input vector consists of the 18 reflectance measurements, the first nine are the bidirectional reflectances of the canopy in the principal plane, from  $+60^{\circ}$  in the backscattering direction to  $-60^{\circ}$  in the forescattering direction at increments of  $15^{\circ}$ , and the remaining nine units represent the bidirectional reflectance across the principal plane (in the same range of interval). The last four inputs correspond to three component signatures, and the solar illumination angle. The three output units consists of the density of the canopy, the crown shape of the trees (the ratio between the radii of the major axis to the minor axis of the crown), and the canopy height (ratio between height to the center of crown to the crown's major radius).

In both contexts, inputs and outputs were transferred to a logarithmic scale. Input data preprocessing was necessary since the reflectance measurements cluster between 0.03 and 0.25. A hyperbolic function is used as the network's activation function. The transformed logarithmic values are scaled between  $-1.0$  and  $1.0$  for the inputs and  $-0.8$  and  $0.8$  for the outputs.

## 4. Neural modelling

### 4.1. Forward modelling: methods and results

In this study we use a feedforward neural network to perform both the forward and the inverse modelling. The neural network approximates the relation between

the inputs and the outputs by means of a supervised learning procedure. Previous studies have shown that such a neural network can approximate any continuous input–output relation to any degree of accuracy, provided it contains sufficient number of hidden units (Hornik *et al.* 1989, Cybenko 1989) and a relationship exists between inputs and outputs. A detailed discussion and review of the multilayer feedforward networks and the algorithm used for training called ‘backpropagation’ is given in Rumelhart *et al.* (1986a, 1986b).

We followed a trial-and-error approach to derive an optimal network. The input layer consists of eight units representing the density, crown shape, height, height distribution within the canopy, sunlit crown signature, sunlit background signature, shaded crown signature, and the solar illumination angle. The output layer consists of 18 units, the first nine representing the bidirectional reflectance of the canopy in the principal plane, from  $+60^\circ$  in the backscattering direction to  $-60^\circ$  in the foreshattering direction at increments of  $15^\circ$ . The remaining nine output units represent the bidirectional reflectance across the principal plane.

Since the number of units in the hidden layer cannot be determined *a priori*, simulations with various network sizes were done. The number of nodes in the hidden layer is varied in increments of 10, between 10 and 50. Training vectors are presented in a random order. Training is terminated when the root mean square error was less or equal to 0.01. A learning rate of 0.3 and a momentum rate of 0.4 are used. Performance of each network is carefully evaluated. A network with one hidden layer consisting of 30 units produced the required degree of accuracy.

The performance of the neural network is measured using  $R^2$  values that are estimated using true values. Performance, in terms of  $R^2$  values for the training data was over 0.9. The predictions and generalizations ability of each network are tested using the testing data set that was not used during the training. Table 3 shows  $R^2$  values between the network predicted reflectance and the actual reflectance generated by the mutual shadowing model.  $R^2$  values of more than 0.96 are achieved for but two of the viewing positions. Thus the neural network is able to learn the relation between the canopy structural parameters, and its bidirectional reflectance fairly well.

#### 4.2. Inverse modelling: methods and results

A multilayer feedforward network with three fully connected layers is developed for the estimation of the three canopy parameters. The network’s input layer consists of 22 units, and the output layer, three units. The input vector consists of the 18 reflectance measurements, nine in each direction as described previously. The last

Table 3. Forward modelling prediction performance using  $R^2$ .

Angle ( $^\circ$ )	Principal plane	Across principal plane
60	0.944	0.984
45	0.933	0.982
30	0.976	0.984
15	0.983	0.984
0	0.982	0.982
-15	0.979	0.984
-30	0.980	0.984
-45	0.980	0.981
-60	0.978	0.984

four inputs correspond to three component signatures and the solar illumination angle. The three units in the output vector represent the density of the canopy, the crown shape of the trees, and the canopy height. The parameters and training strategy in this case are similar to the forward modelling case.

To analyse further the performance of the neural network, three additional networks were developed. Each of the three models was trained using the complete input vector and one output unit representing one of the canopy parameters. The number of the hidden units was not varied between the complete model (three output units) and the three partial models (one output unit.) Training and testing are done as previously described.

Table 4 shows the results of testing the trained network using the testing data set. The table shows the  $R^2$  between the network predicted canopy parameters and the actual canopy parameters used in the simulations. Table 5 shows the results of testing the three networks (for each parameter individually) on the same testing data set. The  $R^2$  for the density parameter was approximately 0.85 and 0.75 for both the crown shape and height parameters.

An interesting issue is to analyse whether a modification or reduction of the input vector affects the performance of the inverse neural network model estimation. This is tested in two different ways. First, the input units representing the bidirectional reflectance across the principal plane are deleted from the input vector. The objective was to test the contribution of the across principal plane inputs in the estimation, as well as to estimate the canopy parameters from the principal plane reflectance only. For this, a new network with the reduced input vector (only 13), a hidden layer of 30 units and an output layer of three units was trained and tested for the estimation of three canopy parameters. Table 6 shows the  $R^2$  of the testing data set for the three

Table 4. Inverse modelling prediction performance using  $R^2$ .

Canopy parameter	$R^2$
Density	0.858
Crown shape	0.759
Height	0.758

Table 5. Inverse modelling prediction performance using  $R^2$  for individual canopy parameters.

Canopy parameter	$R^2$
Density	0.849
Crown shape	0.720
Height	0.744

Table 6. Inverse modelling prediction performance using  $R^2$  for principal plane BRDFs.

Canopy parameter	$R^2$
Density	0.843
Crown shape	0.554
Height	0.526

Table 7. Inverse modelling prediction performance using  $R^2$  for reduced principal plane BRDFs.

Canopy parameter	$R^2$
Density	0.788
Crown shape	0.524
Height	0.552

parameters. The second approach assesses the accuracy of the inversion when the range of the principal plane measurements is reduced. The input vector is modified by deleting the input units that represent the canopy reflectance at  $-60^\circ$  and  $+60^\circ$ . A new network with 11 inputs, 30 hidden units, and three output units is trained and tested on the data sets. Table 7 shows the resulting  $R^2$  of the testing data set. Both approaches estimate density better than crown shape and height.

## 5. Discussion

### 5.1. Forward modelling

Performance results reveal that the neural network model is able to estimate the bidirectional reflectance of different canopies with more than 90% accuracy based on the model. There is no significant difference in the prediction accuracy between the forescattering and the backscattering directions, both in the principal plane and the across principal plane. However, table 3 does reflect lower  $R^2$  values in the principal plane backscattering direction in comparison to the forescattering direction. This is due to the inability of the neural network model to model the hotspot properly. The neural network was not given explicit information about the hotspot.

An analysis of the weights of the hidden layer can reveal the characteristics of the input signal learned by the neural network model in order to make the necessary predictions. Principal component analysis (PCA) has been investigated recently in order to analyse the pattern of weights of a fully trained network (Gopal and Woodcock 1996). In the present study, a covariance matrix of the hidden unit activation (weights) of the trained network was formed and the principal components were extracted. Analysis of the eigen values and eigen vectors in this matrix is useful, in that the eigen values provide an indication of the relative importance of the various principal components.

In the estimation of BRDF, the first four principal components expressed as a correlation between the component and each parameter, are analysed. Table 8 shows

Table 8. Principal component analysis (PLA) eigen values.

Parameter	Component 1	Component 2	Component 3	Component 4
Coverage	0.596	0.145	-0.709	0.167
Crown shape	0.355	-0.360		0.490
Height	0.180	0.865	0.277	0.164
Height variance	0.175	-0.209	0.229	
Sun angle	-0.310			0.755
Sunlit crown signature	-0.597		-0.523	0.150
Sunlit background signature			-0.234	
Shaded background signature		-0.209	0.170	0.336

the eigen vectors of the four components and the proportions of variance explained by each component. Note eigen vectors not significantly different from zero are not shown. An interpretation is made for each of the four principal components.

Principal component 1 represents the general canopy architecture as well as the spatial distribution of the trees within a canopy. The underlying information captured by component 2 represents the general shape of the tree crown. Principal component 3 captures information about the canopy density and the contribution of the sunlit crown portion. The results can be interpreted as follows. The neural network is able to predict that in dense canopies the reflectance from the sunlit tree portion is higher than in sparse canopies where the overall reflectance is from the background soil. Principal component 4 captures the information about the solar illumination geometry and its effect on the proportions (sunlit canopy, sunlit background, shaded canopy) that controls the overall scene reflectance.

This simple analysis of the underlying information captured by the network indicates that canopy structural information, the spatial distribution of crowns in the scene, the solar illumination angle, and the variability of the areas of sunlit and shaded components are influential in predicting the BRDF of any vegetated surface. As demonstrated by component 2, the trees crown shape is an important geometric parameter in determining the canopy's BRDF. This corresponds to findings in prior studies of BRDFs of forest surfaces (Goel and Deering 1985, Kimes 1983, Simmer and Gerstl 1985).

To analyse the neural network predictions of the bidirectional reflectance of a canopy along the principal plane and across the principal plane, and examine the shapes of the model bidirectional reflectance, three canopy sites are studied. The three sites represent typical land cover surfaces of conifer, savanna and shrub. The canopy parameters used in the simulations are from Li and Strahler (1992), but with variations in density and the component signatures. Figures 3, 4 and 5 show a cross-section along the principal plane of the BRDF of the three sites generated by the neural network model. The parameters for each site are shown in table 9.

Each site generates a different BRDF shape. The conifer and shrub sites have wide bowl shapes where as the savanna site shows a dome shaped BRDF. In both the conifer and shrub sites, the trees present a wide cross-section towards a viewing sensor and the bidirectional reflectance increases when the sensor off-nadir view

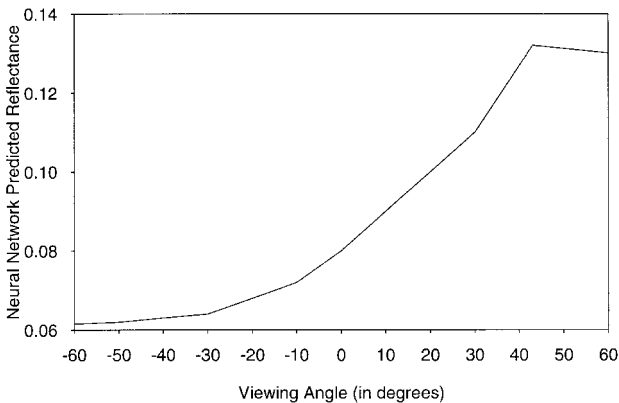


Figure 3. Neural network model BRDF in the principal plane of the conifer site.

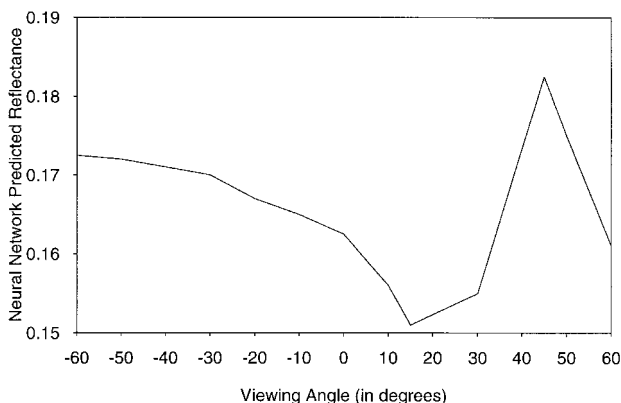


Figure 4. Neural network model BRDF in the principal plane of the savanna site.

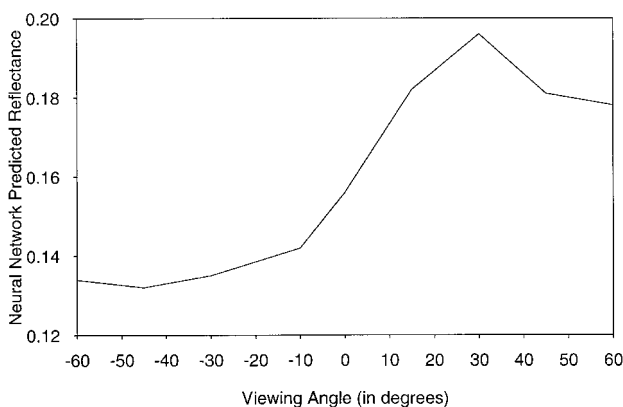


Figure 5. Neural network model BRDF in the principal plane of the shrub site.

Table 9. Parameters used for simulating conifer, savanna, and shrub sites.

Site	Coverage	Height	Crown major radius	Crown minor radius	Sun angle
Conifer	70%	20·00	10·00	3·00	55·00
Savanna	99%	12·50	2·50	5·00	45·00
Shrub	2%	0·50	0·50	0·25	24·00

angle increases towards the horizon. In such situations the trees obscure more of their dark shadows falling on the background within the vegetation stand (Li and Strahler 1992). The savanna site in figure 4 shows an opposite BRDF shape. The general shape of the BRDF shows a dome shape as the trees are rather broad and present their greatest cross-section when a viewing sensor is overhead. As the viewing sensor descends towards the horizon and assumes large off-nadir angles more shadows are revealed, and consequently the overall scene reflectance decreases. This shows that the general shape of the BRDF is highly controlled by the shape of the trees.

The solar illumination angles for the three sites are 55°, 45°, and 24°. Note that

the neural network model is trained to predict the bidirectional reflectance at specific viewing angles and  $55^\circ$  and  $24^\circ$  are not synonymous with these angles. Hence the neural network model predictions do not show the exact location of the hotspot, but shows the highest reflectance at the closest prediction angle. This is not the case for the second test site in figure 4, where the solar illumination angle matched the neural network model prediction angles. Had the prediction angles matched in the other sites, a clearer hotspot would have been displayed. A finer interval for the viewing angles may have resulted in more accurate predictions. The ultimate goal of neural network modelling is to generalize outside of the training data set. Hence in this study, the fully trained neural network is tested on unseen field data that is part of the Oregon Transect Ecosystem Research Project (OTTER).

### 5.2. Forward model validation

The prediction ability of the neural network model can be examined by comparing the shape of the BRDF along the solar principal plane and actual directional reflectance measurements collected by the Advanced Solidstate Array Spectrometer (ASAS) (Irons *et al.* 1991). The experimental targets are the conifer stands along the Oregon Transect that were imaged by ASAS. As the reflectance measurements are collected over various sites with different canopy structures and varying densities, the neural network model can be validated in canopies with different characteristics.

The Oregon test sites lie on a west-to-east transect, along a temperature and moisture gradient that produces a large variation in ecosystem structure and function (Runyon *et al.* 1993). It offers a wide range of leaf area index, and the understory vegetation is composed of varying proportions of shrubs, grasses and ferns with some exposed soil. Four sites are used in the validation process—Metolius, Waring's Woods, Cascade Head, and Scio. The canopy characteristics of each site are shown in table 10.

Figure 6 shows a cross-section along the solar principal plane for the four test sites as predicted by the neural network model (—) and as captured by ASAS red band (16) (⋯). Note that ASAS imagery is limited to  $-45^\circ$  to  $45^\circ$  while the model predictions span a larger interval from  $-60^\circ$  to  $60^\circ$ . The discussion will be limited to the common interval only. ASAS measurements are shown as signal values (in  $\text{mW cm}^{-2} \text{sr}^{-1} \mu\text{m}^{-1}$ ) and not as absolute reflectance values. This is because upon converting the ASAS brightness to units of radiance for the red band (16), the calculated radiances were far lower than the path radiances predicted by an atmospheric correction model (Abuelgasim and Strahler 1994). This anomalous result is most likely due to incorrect calibration of the ASAS detectors. Band 16 is centred near the chlorophyll absorption maximum and hence, the signal received by the ASAS in band 16 is typically very low for vegetated targets. The detectors fitted to

Table 10. Canopy characteristics of the OTTER sites.

Site	Coverage	Mean height	Mean crown shape	Sun angle
Metolius	44%	9.24	2.88	47.50
Waring woods	31%	38.89	6.65	22.40
Cascade Head	68%	47.64	6.10	22.20
Scio	87%	28.01	5.00	52.50

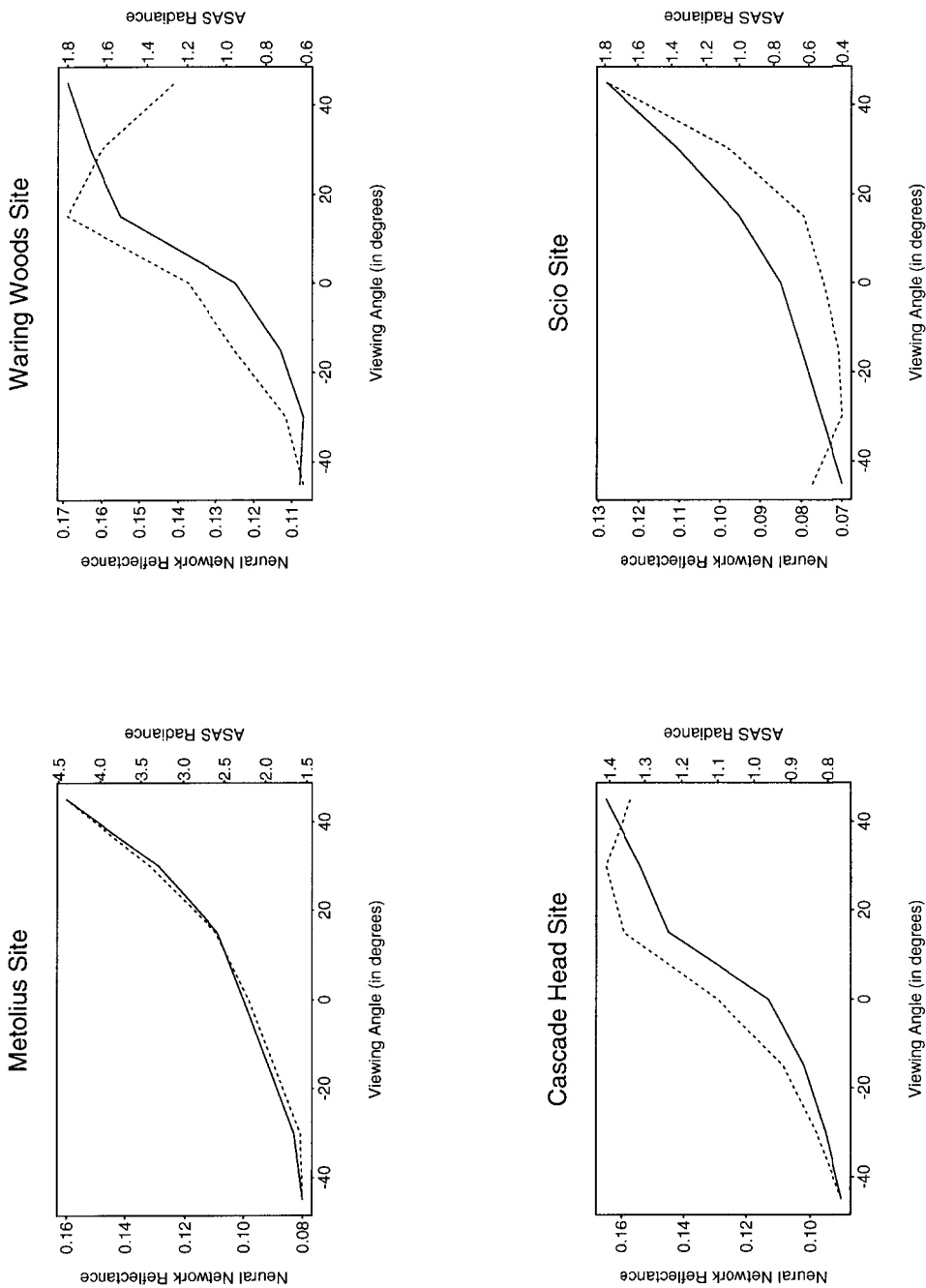


Figure 6. Comparison between the Oregon Transect Ecosystem Research Project (OTTER) sites BRDF and the neural network predicted BRDF along the principal plane.

ASAS for this mission did not behave well at low signal levels due to low responsivity. For these reasons, the comparison is restricted to the BRDF shape only.

For the Waring Woods and Cascade Head sites the shape predicted by the neural network model fits the ASAS radiance curves fairly well. The plots show that the hotspot is not well captured by the neural network model compared to the ASAS measurements. Note that the model is trained to predict the BRDF at specific viewing angles, and the hotspot locations for these sites are not among the prediction angle of the model. Hence a smooth line between any two model prediction angles would unlikely show the hotspot. For these sites the sun angle during the ASAS overpass was approximately  $22^\circ$ , and both the neural network model curves and the ASAS curves assumed the hotspot position at the closest prediction/viewing angle. The hotspot peak captured by the neural network model is not apparent in the ASAS curves for the Scio and Metolius sites. The sun angle at the time of the ASAS overpass ( $52^\circ$  for Scio and  $47^\circ$  for Metolius) is greater than the maximum look angle of the ASAS at  $45^\circ$ , and is thus beyond its field of view, though the ASAS curves shows tendency of higher reflectance at the hotspot image.

The BRDF bowl shape for the Metolius, Waring Woods, and Cascade Head sites is predicted fairly well. For the Scio site, the ASAS radiance curves shows an accentuated bowl shape that is not emphasized by the corresponding neural network model. The bowl shape of the BRDF is highly influenced by the mutual shadowing effect within the canopy. The input vector for the neural network did not contain a parameter to describe this effect, and perhaps this may be a primary reason for the lack of fit. The conclusion to be drawn from this analysis is that the neural network model is able to predict the correct shape of the BRDF but not the location of the hotspot. Additional parameters such as mutual shadowing may have to be incorporated in future research to overcome the limitation of the present approach.

### 5.3. Inverse modelling

The inversion results from the  $R^2$  worked fairly well for all the three canopy parameters, both individually and jointly, capturing 75% to 85% of the variance (tables 4 and 5). The density parameter had the highest  $R^2$  value of 0.85 and is thus the best estimated parameter. There is no significant difference in the accuracy of the estimation of the crown shape ( $R^2$  is 0.75) and the canopy height ( $R^2$  is 0.75). Similarly, there is no significant difference between the estimation of the parameters individually or jointly.

The results presented in table 6 have shown that there is a decrease in the accuracy of the estimation of crown shape and the canopy height when the across principal plane bidirectional reflectance measurements are excluded, while there is no change in the accuracy of the density parameter. It can be inferred that principal plane bidirectional reflectance solely is not enough to explain fully the variance in the distribution of the angular reflectance above the canopy. Across principal plane bidirectional reflectance adds valuable information and is thus necessary to be included for properly modelling the inverse relation.

A similar decline in the accuracy for all the three canopy parameters was noted when the principal plane measurements were decreased from a range of  $-60^\circ$  to  $+60^\circ$  to a range of  $-45^\circ$  to  $+45^\circ$  (see table 7). Perhaps a wider range along the principal plane measurements may lead to better inversion results.

## 6. Conclusion

This study demonstrates that neural networks can be effective in forward and inverse canopy modelling. The forward modelling paradigm proves that such networks are able to capture the necessary information needed to predict the BRDF of forest surfaces. The neural network model exploits and learns the relation between the canopy form parameters, canopy density, and viewing and illumination positions. Analysis of the weight matrix between the input layer and the hidden layer reveals the underlying information captured by the network to model the BRDF of a forest canopy. An accurate inversion of canopy structural parameters from a canopy bidirectional reflectance can be achieved through the use of a multi-layer feedforward neural network. As the inversion procedure has worked fairly well for certain canopy parameters, this technique may likely be extended to include other canopy parameters such as leaf area index (LAI). The input vector to the neural network contains information about the BRDF in the principal plane and across the principal plane only. Since the information in the BRDF generated by the Li and Strahler model is not uniformly distributed, the principal plane and the across principal plane may not contain all the information of a canopy BRDF. This study has demonstrated that neural network models are sensitive to the choice of the input vector. A reduction in prediction accuracy is noted when the input vector does not contain critical parameters. Hence, if the input vector contained more information from other azimuthal directions, the neural network model may have made better predictions.

The ideal scenario for performing an inversion strategy is the use of a comprehensive data set that relates canopy structural parameters and biophysical characteristics to the canopy bidirectional reflectance. However, such a data set does not exist and would be difficult and expensive to collect. It was thus necessary to simulate the data set using an existing canopy reflectance model. In this respect, the inversion strategy using a simulated data set presents a slightly less difficult inversion scenario. Actual measurements of a signal received by a remote sensor carries with it the signatures of other external factors such as soil and atmosphere, and also stochastic elements such as wind and dew (Goel 1989). In this case the effect of the noise can complicate the inversion process and might affect the estimated canopy parameters.

However, the primary objectives of the study are to explore the potentials offered by neural networks in canopy modelling. Most canopy inversion strategies try to minimize an error function of measured and observed canopy reflectance using least squares techniques (Goel and Thompson 1985). Multilayer feedforward neural networks, trained by the backpropagation algorithm, is currently the most popular optimization procedure to minimize the error function. The learning algorithm is simple, and can thus be applied easily for learning a relationship between a set of input vectors and a set of output parameters. Neural network models provide an additional technique for inverse canopy modelling and have proved to be well suited for inversion of remotely sensed data. One major advantage of such networks is that they learn adaptively by examples to approximate an input–output relation or a mapping function between the input and output data, without any *a priori* knowledge of this function.

## Acknowledgment

The forward modelling was carried out using BRDF modelling software developed by P. Lewis, University College London, into which the Li and Strahler model was incorporated by W. Wanner, Boston University, utilizing code written

by C. Schaaf; the software was written as part of NASA's EOS-MODIS project (NAS5-3/369). The AMBRALS software is available from W. Wanner. We appreciate the help and support of P. Lewis, W. Wanner, and C. Schaaf in this respect. We greatly appreciate the many insightful suggestions provided by Dr Xiaowen Li.

## References

- ABUELGASIM, A. A., and STRAHLER, A. H., 1994, Modelling bidirectional radiance measurements collected by the Advanced Solid-state Array Spectroradiometer ASAS over Oregon transect conifer forests. *Remote Sensing of Environment*, **47**, 261–275.
- CHANDRASEKHAR, S., 1950, *Radiative Transfer* (London: Oxford University Press).
- CYBENKO, G., 1989, Approximation by superpositions of sigmoidal function. *Mathematics of Control, Signals, and Systems*, **2**, 303–314.
- GERSTL, S. A. W., SIMMER, A. C., and POWERS, B. J., 1986, The canopy hot-spot as crop identifier. In *Symposium on Remote Sensing for Resources Development and Environmental Management, August 1986* (Enschede: FRG), pp. 261–263.
- GOEL, N. S., 1987, Models of vegetation canopy reflectance and their use in estimation of biophysical parameters from reflectance data. *Remote Sensing Reviews*, **3**, 1–212.
- GOEL, N. S., 1989, Inversion of canopy reflectance models. In *Theory and Applications of Optical Remote Sensing*, edited by G. Asrar (New York: Wiley), pp. 205–251.
- GOEL, N. S., and DEERING, D. W., 1985, Evaluation of a canopy reflectance model for LAI estimation through its inversion. *Institute for Electrical and Electronic Engineers Transactions in Geosciences and Remote Sensing*, **23**, 674–684.
- GOEL, N. S., and THOMPSON, R. L., 1985, Optimal solar/viewing geometry for an accurate estimation of leaf area index and leaf angle distribution from bidirectional canopy reflectance data. *International Journal of Remote Sensing*, **6**, 1493–1520.
- GOPAL, S., and WOODCOCK, C. E., 1996, Remote sensing of forest change using artificial neural networks. *Institute for Electrical and Electronic Engineers Transactions in Geosciences and Remote Sensing*, **34**, 398–404.
- HORNİK, K., STINCHCOMBE, M., and WHITE, H., 1989, Multilayer feedforward networks are universal approximators. *Neural Networks*, **2**, 359–366.
- IRONS, J. R., RANSON, K. J., WILLIAMS, D. L., IRISH, R. R., and HUEGEL, F. G., 1991, An off-nadir pointing imaging spectroradiometer for terrestrial ecosystem studies. *Institute for Electrical and Electronic Engineers Transactions in Geosciences and Remote Sensing*, **29**, 66–74.
- KIMES, D. S., 1983, Dynamics of directional reflectance factor distributions for vegetation canopies. *Applied Optics*, **22**, 1364–1372.
- KIMES, D. S., 1991, Radiative transfer and vegetation canopies. In *Photon-Vegetation Interactions*, edited by R. B. Myneni and J. Ross (Berlin: Springer-Verlag), pp. 339–388.
- KIMES, D. S., and SMITH, J. A., 1980, Simulation of solar radiation absorption in vegetation canopies. *Applied Optics*, **19**, 2801–2811.
- KUUSK, A., 1985, The hot spot effect of a uniform vegetation cover. *Soviet Journal for Remote Sensing*, **3**, 645–658. In Russian.
- LI, X., and STRAHLER, A. H., 1985, Geometric-optical modelling of a conifer forest canopy. *Institute for Electrical and Electronic Engineers Transactions in Geosciences and Remote Sensing*, **23**, 705–721.
- LI, X., and STRAHLER, A. H., 1986, Geometric-optical bidirectional reflectance modelling of a conifer forest canopy. *Institute for Electrical and Electronic Engineers Transactions in Geosciences and Remote Sensing*, **24**, 906–919.
- LI, X., and STRAHLER, A. H., 1992, Geometric optical bidirectional reflectance modelling of the discrete crown vegetation canopy. Effect of crown shape and mutual shadowing. *Institute for Electrical and Electronic Engineers Transactions in Geosciences and Remote Sensing*, **30**, 276–292.
- MARSHAK, A. L., 1989, The effect of the hot spot on the transport equation in plant canopies. *Quantitative Spectroscopy and Radiative Transfer*, **42**, 615–630.
- MYNENI, R. B., and ROSS, J., 1991, *Photon-Vegetation Interactions* (Berlin: Springer-Verlag).
- MYNENI, R. B., ASRAR, G., and GERSTL, S. A. W., 1990, Radiative transfer in three dimensional leaf canopies. *Transport Theory and Statistical Physics*, **19**, 205–250.

- MYNENI, R. B., MARSHAK, A., KNYAZIKHIN, Y., and ASRAR, G., 1991, Discrete ordinates method for photon transport in leaf canopies. In *Photon-Vegetation Interactions*, edited by R. B. Myneni and J. Ross (Berlin: Springer-Verlag), pp. 45–109.
- NILSON, T., 1977, A theory of radiation penetration into non-homogeneous plant canopies. In *The Penetration of Solar Radiation into Plant Canopies* (Tartu: Academy of Sciences, ESSR), pp. 5–70. In Russian.
- NILSON, T., and KUUSK, A., 1989, A reflectance model for the homogeneous plant canopy and its inversion. *Remote Sensing of Environment*, **27**, 157–167.
- NILSON, T., and PETERSON, U., 1991, A forest canopy reflectance model and test case. *Remote Sensing of Environment*, **37**, 131–142.
- PIERCE, L. E., SARABANDI, K., and ULABY, F. T., 1994, Application of an artificial neural network in canopy scattering inversion. *International Journal of Remote Sensing*, **15**, 3263–3270.
- ROSS, J., and MARSHAK, A., 1991, Monte Carlo methods. In *Photon-Vegetation Interactions*, edited by R. B. Myneni and J. Ross (Berlin: Springer-Verlag), pp. 441–467.
- RUMELHART, D. E., HINTON, G. E., and WILLIAMS, R. J., 1986a, Learning representations by back-propagating errors. *Nature*, **323**, 533–536.
- RUMELHART, D. E., HINTON, G. E., and WILLIAMS, R. J., 1986b, Learning internal representations by error propagation. In *Parallel Distributed Processing: Exploration in the Microstructure of Cognition. Volume 1, Foundations*, edited by D. E. Rumelhart, J. L. McClelland and the PDP research Group (Cambridge, MA: The MIT Press), pp. 318–362.
- RUNYON, J., WARING, R. H., and GOWARD, S. N., 1993, Environmental limits on net primary production and light-use efficiency across the Oregon transect. *Ecological Applications*, **42**, 226.
- SIMMER, C., and GERTSL, S. A. W., 1985, Remote sensing of angular characteristics of canopy reflectances. *Institute for Electrical and Electronic Engineers Transactions in Geosciences and Remote Sensing*, **23**, 648–658.
- SMITH, J. A., 1993, LAI inversion using a backpropagation neural network trained with multiple scattering model. *Institute for Electrical and Electronic Engineers Transactions in Geosciences and Remote Sensing*, **31**, 1102–1111.
- SMITH, J. A., and OLIVER, E. E., 1974, Effects of changing canopy directional reflectance of feature selection. *Applied Optics*, **13**, 1599–1604.
- STRAHLER, A. H., WOODCOCK, C. E., and SMITH, J. A., 1986, On the nature of models in remote sensing. *Remote Sensing of Environment*, **20**, 121–139.
- WANNER, W., STRAHLER, A. H., HU, B., MULLER, J.-P., LI, X., BARKER SCHAFF, C. L., and BARNESLEY, M. J., 1997, Global retrieval of bidirectional reflectance and albedo over land from EOS MODIS and MISR data: theory and algorithm, *Journal of Geophysical Research*, **102**, 17143–17161.
- ZURK, L. M., DAVIS, D., NJOKU, L., TSANG, L., and HWANG, J. N., 1992, Inversion of parameters for semi-arid regions by a neural network. *Proceedings of the International Geosciences and Remote Sensing Symposium (IGARSS 92): Volume 2, Houston, TX* (New York: Institute for Electrical and Electronic Engineers), pp. 1075–1078.